BRIDGED DELAMINATION CRACKS IN CURVED BEAMS AND MIXED-MODE BENDING SPECIMENS

Roberta Massabò [1] and Brian N. Cox [2]

[1] *Department of Structural and Geotechnical Engineering, University of Genova, Via Montallegro 1, 16145, Genova, Italy*
[1] *Rockwell Science Center, 1049 Camino Dos Rios, Thousand Oaks, CA 91360, U.S.A.*

SUMMARY: Theoretical approaches based on bridged-crack models and plate/beam theory have proved to be effective in the modeling of Mode I and Mode II delaminations in composite laminates reinforced through the thickness. This paper deals with some aspects of the modeling of Mixed Mode delaminations. Two typical mixed mode problems are considered: the curved beam in bending (C specimen) and the Mixed-Mode Bending specimen (MMB) reinforced through the thickness.

KEYWORDS: delamination, mixed mode, stitching, energy release rate, crack bridging, beam theory.

INTRODUCTION

Through-thickness reinforcement is widely accepted as the most efficient method of solving the problem of delamination in composite laminates. It is typically applied by stitching or weaving continuous fibers tows or inserting discontinuous rods (z-reinforcements). Experimental tests and theoretical analyses carried out during the last 20 years have shown that the new technology of through-thickness reinforcement produces materials with a damage tolerance/resistance that is adequate also for load bearing structures.

Theoretical approaches based on bridged-crack models and plate/beam theory have proved to be effective in modeling the Mode I and Mode II delamination of composite laminates reinforced through the thickness [1-5]. However, delaminations in real structures are typically in mixed mode conditions. It is then important to formulate models that can describe the performance of the through-thickness reinforcement in structures subject to mixed mode loading.

This paper deals with some aspects of the theoretical modeling of mixed mode delamination processes. Two different problems are examined, the C specimen and the Mixed-Mode Bending specimen (MMB). The C specimen is a delaminated curved structure loaded in bending. A method to define the strain energy release rate and the mode mixture based on beam theory will be presented. The Mixed-Mode Bending specimen is a delaminated beam loaded in such a way that Mode I (DCB type) and Mode II (ENF type) loadings are simultaneously applied [5]. Some preliminary results of a bridged-crack model formulated to

analyze delamination crack growth in MMB specimens reinforced through the thickness will be presented.

MIXED MODE DELAMINATION IN COMPOSITE LAMINATES

Mixed Mode Delamination in Curved Beams in Bending

Figure 1.a shows a C specimen loaded by bending moments M. The mean radius of curvature of the specimen is r_m and the thickness is $2h = r_0$-r_i, with r_0 and r_i the outer and inner radii. A circular through-thickness crack of length $2a$ lies along the circumferential plane of radius r_c and subtends an angle $2\theta_c$ in the system of cylindrical coordinates r-θ-z. The material is homogeneous, orthotropic with cylindrical anisotropy and pole O, and linearly elastic. The specimen is in plane strain conditions normal to the axis z and M is the moment per unit width.

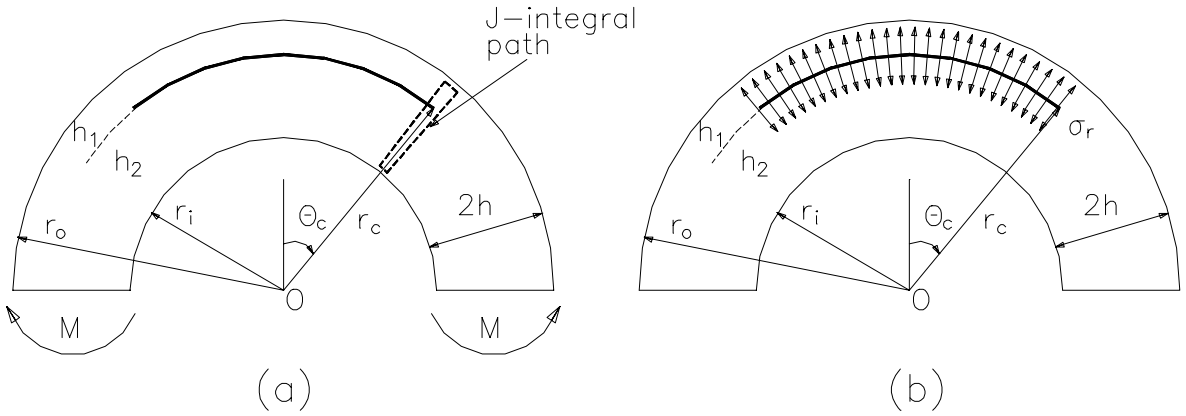

Fig. 1: a) C specimen and conventions. b) Geometry used in the superposition scheme.

Lu et al. [7] studied the C specimen using the finite element method (FEM) and curved beam theory. They also analyzed the specimen by FEM in the presence of through thickness reinforcement [8]. They concluded that beam theory is able to capture the main trends of the solution, but leads to predictions which differ from those of the finite element method even when the relative curvature of the specimen is small ($h/r_m = 0.1$) and the specimen is isotropic. Massabò and Cox [9] reconsidered the application of curved beam theory. They found that for the relative curvatures which are typically used ($h/r_m \leq 0.5$), low degrees of orthotropy and long enough initial crack lengths, more general beam theory solutions than those considered by Lu and Hutchinson do after all agree with rigorous 3D elasticity solutions. They proposed a method, similar to that proposed by Williams [10] for straight beams, for easily calculating the strain energy release rate in curved beams. They also defined a procedure to calculate the mode mixture at the tip of the delamination by extending the results of Suo [11] to curved beams. Here their results will be briefly recalled and discussed.

The problem of Fig.1.a is solved by superposing the solution of the problem shown in Fig. 1.b on that of a curved beam with no crack subject to bending moments M. The radial stress σ_r applied along the crack faces in Fig. 1.b is the tensile radial stress component generated by M in the intact specimen at the plane defined by r_c [12].

The problem of Fig. 1.b is solved through elementary beam theory by referring to a unit width of the body (z direction) and using the reduced modulus $E'_\theta = E_\theta/(1-\nu_{r\theta}\nu_{\theta r})$ in the place of the longitudinal modulus E_θ. The displacement field is defined by the longitudinal displacement, u_s, the radial displacement, u_r, and the bending rotation, φ, on the center plane of the beam; the stress field by the stress resultants over a unit width, namely the normal force, N, bending moment, M, and shear force, Q (the sign convention following classical beam theory). The longitudinal deformation (stretching), shear deformation and total curvature on the center plane are denoted by ε, γ and χ. The model retains all the assumptions of curved beam theory and accounts for shear deformations. Compatibility, equilibrium and constitutive equations are presented in the Appendix of [9]. The constitutive response is characterized by coupling between stretching and bending and between curvature and normal force.

Due to symmetry, only the part of the structure for $\theta \geq 0$ needs be examined and is represented by three beams rigidly joined at $\theta = \theta_c$. The depths of the beams are h_1, h_2 and $h_3 = 2h$ and the mean radii $r_1 = r_c + h_1/2$, $r_2 = r_c - h_2/2$ and $r_3 = r_m$. Beams 1 and 2 are defined for $0 \leq \theta \leq \theta_c$ and beam 3 for $\theta \geq \theta_c$. Uniformly distributed radial loads act along the centerlines of beams 1 and 2, $p_{r1} = -\sigma_r r_c/r_1$ and $p_{r2} = \sigma_r r_c/r_2$.

The constitutive and equilibrium equations for the three beams and the boundary and continuity conditions for stress resultants and generalized displacements (at $\theta = \theta_c$) define a linear boundary value problem. The problem is solved in closed form [9] and the crack opening and sliding displacements are then calculated as $2u_r = u_{r2} - u_{r1}$ and $2u_s = u_{s2} - \varphi_2(r_3 - r_2) - u_{s1} - \varphi_1(r_1 - r_3)$.

Strain Energy Release Rate

The strain energy release rate, G, of the structure of Fig. 1.a is most conveniently defined by calculating the J-integral along a path surrounding the crack tip [13]. A new expression for the J-integral applicable when the direction of crack advance is a curved path has been proposed in [9]. If the path shown by dashed lines in Fig. 1.a is considered and the elastic strain energy is defined in terms of stress resultants, $J = \mathsf{G}$ takes the form:

$$\mathsf{G} = \frac{1}{r_c}\left\{\frac{1}{2}\sum_{i=1}^{2} r_i\left(\frac{N_{Ri}^2}{E'_\theta A_i} + \frac{M_i^2}{E'_\theta J_{Ri}} + \frac{T_i^2}{G_{r\theta} K_{Ri}}\right) - \frac{1}{2} r_3\left(\frac{N_{R3}^2}{E'_\theta A_3} + \frac{M_3^2}{E'_\theta J_{R3}} + \frac{T_3^2}{G_{r\theta} K_{R3}}\right)\right\} \quad (1)$$

where $G_{r\theta}$ is the shear modulus in the plane r-θ, A_i is the cross-sectional area of the ith beam, $A_i = h_i$, J_{Ri} the reduced moment of inertia, $J_{Ri} = m_i(2h_i)^3/12$, and K_{Ri} the reduced shear rigidity, $K_{Ri} = 5/6 m_{Qi} A_i$; m_i and m_{Qi} depend on the relative curvature of the ith beam and are very close to unity for $h/r_i < 0.1$ [14]. In the loading configuration of Fig. 1.b the second term in curved brackets on the right hand side of Eq. (1) vanishes.

The reduced normal force N_{Ri} in Eq. (1) is defined as a function of the normal force and the bending moment, $N_{Ri} = N_i - M_i/r_i$. Its introduction leads to the compact form of G presented in Eq. (1), which is very similar to that used to describe a straight beam. As we will see this form proves to be particularly useful in the partitioning of the modes. The strain energy release rate of Eq. (1) reduces to that obtained by Williams [10] in the case of a straight beam with $r_i/r_c = 1$, $J_{Ri} = J_i$, $K_{Ri} = K_i$ and $N_{Ri} = N_i$ (i=1,…,3).

Equation (1) can also be applied to a generic (noncircular) curved beam in the presence of through thickness reinforcements or other bridging mechanisms, provided all the quantities in the equation represent the actual condition at the crack tip. The radii r_i (i=1,..,3) and r_c, for instance, must represent the local radii of the beams and the local radius of the crack at its tip.

Figures 2.a and 2.b depict the dimensionless strain energy release rate, $\mathcal{G}E'_\theta(2h)^3/M^2$, as a function of the angle subtended by the crack, θ_c, for three different positions of the crack, h_1/h_2 = 1, 1/3 and 3 and for two different relative curvatures, h/r_m= 0.1 (r_i/r_0 = 4/5) and h/r_m= 0.5 (r_i/r_0 = 2/3). The curves are compared with the FEM results of Lu et al. for an isotropic material [7]. It can be seen that, apart from small values of θ_c for which a two-dimensional analysis is required, beam theory predictions are fairly accurate.

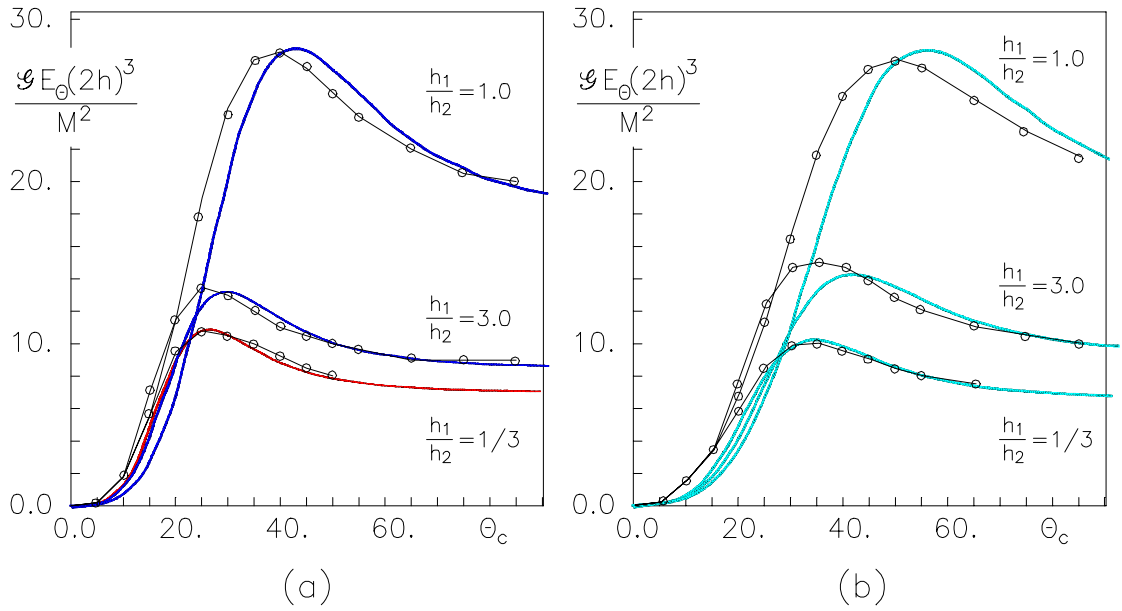

Fig.2: Dimensionless strain energy release rate in an isotropic C specimen as a function of the angle subtended by the crack (thick lines: beam theory; thin lines: FEM [7]). a) Relative curvature h/r_m= 0.1 (r_i/r_0 = 4/5). b) Relative curvature h/r_m= 0.5 (r_i/r_0 = 2/3).

Mode Decomposition and Stress Intensity Factors

If N_3, M_3 and T_3 are zero, Eq. (1) can be modified to the following form by introducing $\beta = h_1/r_c$ and $\eta=h_1/h_2$:

$$\mathcal{G} = \frac{1}{2E'_\theta}\left\{\frac{N_{R1}^2}{h_1 A_{cu}} + \frac{M_1^2}{h_1^3 I_{cu}} - \frac{2M_1 N_{R1}}{h_1\sqrt{A_{cu} I_{cu}}}\sin\gamma_{cu}\right\} \qquad (2)$$

where A_{cu}, I_{cu} and $\sin\gamma_{cu}/(A_{cu}I_{cu})^{0.5}$ are parameters depending on the geometry of the beam defined in [9]. In Eq. (2) the contributions to $\mathcal{G}$ from the shear resultants have been neglected and N_{R2} and M_2 defined as functions of N_{R1} and M_1 through equilibrium, $N_{R2} = -N_{R1}r_1/r_2$ and $M_2 = -M_1r_2/r_1+N_{R1}(r_1-r_2)$. If N_3, M_3 and T_3 are not zero, the superposition method proposed by Suo [11] can be applied and N_i, M_i and T_i (i=1,2) redefined in such a way as to cancel the i=3 components.

The strain energy release rate in an orthotropic material can also be defined as a function of the stress intensity factors at the crack tip [11]:

$$\mathsf{G} = \frac{n}{E'_\theta}(\lambda^{-3/4}K_{\mathrm{I}}^2 + \lambda^{-1/4}K_{\mathrm{II}}^2) \tag{3a}$$

$$n = \sqrt{\frac{1+\rho}{2}}, \quad \lambda = \frac{E'_r}{E'_\theta}, \quad \rho = \frac{\sqrt{E'_\theta\, E'_r}}{2G_{r\theta}} - \sqrt{\nu'_{\theta r}\, \nu'_{r\theta}} \tag{3b}$$

The right hand sides of Eqs. (2) and (3a), which define the same quantity G, can be considered as the absolute values of two complex numbers and equated:

$$\sqrt{n}\left|\lambda^{-3/8}K_{\mathrm{I}} + i\lambda^{-1/8}K_{\mathrm{II}}\right| = \frac{1}{\sqrt{2}}\left|\frac{-N_{\mathrm{R1}}}{\sqrt{h_1 A_{\mathrm{cu}}}} - ie^{i\gamma_{\mathrm{cu}}}\frac{M_1}{\sqrt{h_1^3 I_{\mathrm{cu}}}}\right| \tag{4}$$

Consequently the two complex numbers will differ only by a phase angle shift, $\omega_{cu} = \omega_{cu}(\rho, \eta, \lambda)$:

$$\sqrt{n}(\lambda^{-3/8}K_{\mathrm{I}} + i\lambda^{-1/8}K_{\mathrm{II}}) = \frac{e^{i\omega_{\mathrm{cu}}}}{\sqrt{2}}\left(\frac{-N_{\mathrm{R1}}}{\sqrt{h_1 A_{\mathrm{cu}}}} - ie^{i\gamma_{\mathrm{cu}}}\frac{M_1}{\sqrt{h_1^3 I_{\mathrm{cu}}}}\right) \tag{5}$$

The Mode I and Mode II stress intensity factors are easily defined from Eq. (5):

$$\begin{aligned} K_{\mathrm{I}} &= \frac{\lambda^{3/8}}{\sqrt{2n}}\left[\frac{-N_{\mathrm{R1}}}{\sqrt{h_1 A_{\mathrm{cu}}}}\cos\omega_{\mathrm{cu}} + \frac{M_1}{\sqrt{h_1^3 I_{\mathrm{cu}}}}\sin(\omega_{\mathrm{cu}} + \gamma_{\mathrm{cu}})\right] \\ K_{\mathrm{II}} &= \frac{\lambda^{1/8}}{\sqrt{2n}}\left[\frac{-N_{\mathrm{R1}}}{\sqrt{h_1 A_{\mathrm{cu}}}}\sin\omega_{\mathrm{cu}} - \frac{M_1}{\sqrt{h_1^3 I_{\mathrm{cu}}}}\cos(\omega_{\mathrm{cu}} + \gamma_{\mathrm{cu}})\right] \end{aligned} \tag{4}$$

The phase angle shift $\omega_{cu} = \omega_{cu}(\rho, \eta, \lambda)$ can be defined through a rigorous solution of the problem. For a straight beam Suo and Hutchinson [15] showed that the phase angle shift does not depend on λ, since both sides of Eq. (3) are independent of λ. They also derived ω=49.1 deg. for η=1 and ω=52.1-3η deg. for ρ=1 (isotropy), and showed that ω=52.1-3η deg. is an excellent approximation for a wide range of ρ.

Figures 3.a and 3.b show the relative amount of Mode II to Mode I defined by the phase angle $\Psi = \tan^{-1}(K_{\mathrm{II}}/K_{\mathrm{I}})$ as a function of the angle subtended by the crack, θ_c, calculated through Eq. (4) using the straight beam approximation for ω_{cu}. The cases examined represent two isotropic beams with relative curvatures h/r_m= 0.1 and 0.5, and h_1/h_2 = 1. The results are compared with the finite element results of Lu et al. [7]. The relative amount of Mode II to Mode I increases almost linearly with θ_c. Beam theory predictions are accurate for the entire range of θ_c apart from very small values (short cracks), for which the crack will be approximately in Mode I and K_I equal to that of a crack in an infinite medium [16].

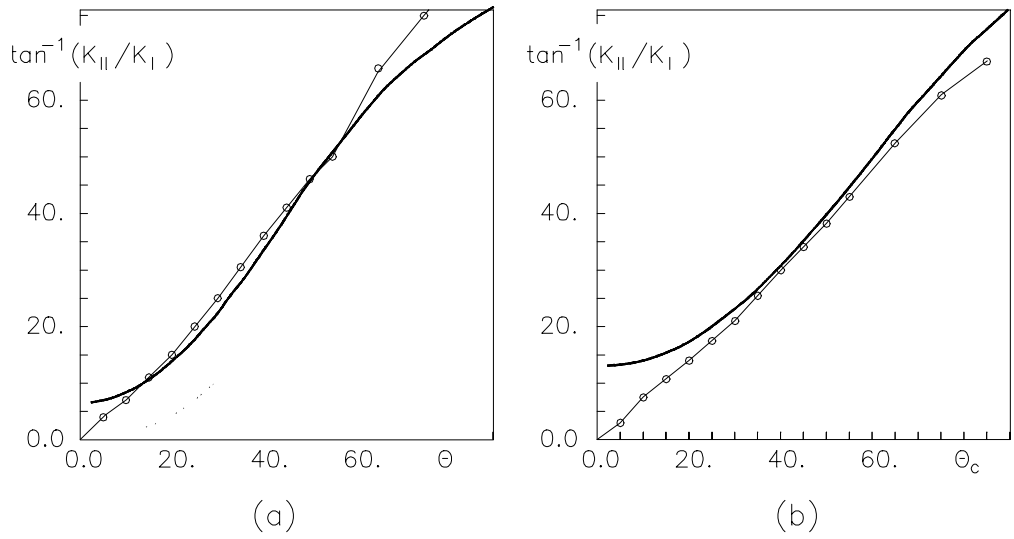

Fig.3: Measure of the relative amount of Mode II to Mode I in the C specimen ($h_1/h_2 = 1$) as a function of the angle subtended by the crack (thick lines: beam theory; thin lines: FEM [7]). a) Relative curvature $h/r_m = 0.1$. b) Relative curvature $h/r_m = 0.5$.

Mixed Mode Delamination in MMB Specimens Reinforced Through the Thickness

The Mixed-Mode Bending test apparatus is shown schematically in Fig. 4.a. The specimen is a thin laminate symmetric about its mid-plane with span $2L$, thickness $2h$, width b and a mid-plane delamination of length a (L, $a >> h$). The test combines the DCB (Mode I) and the ENF (Mode II) tests. The MMB test is now the most popular test for mixed mode toughness characterization of conventional (2D) polymer matrix composites. Depending on the position of the load applied along the rigid lever, a complete range of mixed mode conditions at the crack tip can be achieved. Moreover, in the absence of bridging mechanisms, the test maintains a fairly constant mixed mode ratio as the delamination grows along the mid-plane. The toughness, $\mathcal{G}_C$, is typically defined from the value of the load at crack initiation using a corrected beam theory [17-19] and it depends on the amount of Mode II to Mode I loading acting on the delamination, $\mathcal{G}_C = \mathcal{G}_C(\mathcal{G}_I,\mathcal{G}_{II})$, $\mathcal{G}_I$ and $\mathcal{G}_{II}$ being the Mode I and Mode II components of the strain energy release rate.

The advantages of the MMB test over other mixed mode tests make it a good candidate for the mixed mode fracture characterization of laminates reinforced through the thickness. The fracture behavior of these materials, however, is not only controlled by $\mathcal{G}_C(\mathcal{G}_I,\mathcal{G}_{II})$ but also strongly depends on the bridging mechanisms developed by the through-thickness reinforcements during crack growth in the so called large-scale bridging regime. Through-thickness reinforcements bridging a delamination shield the tip from the applied loads by imposing tractions $\boldsymbol{p}$ across the crack. In plane problems, $\boldsymbol{p} = \boldsymbol{p}(u_3,u_1)$ depend on the opening and sliding displacements along the crack, u_3 and u_1, where x_3 is the through-thickness direction and x_1 is the direction of crack propagation (see Fig. 4.b). Once the bridging law of the reinforcement, $\boldsymbol{p}(u_3,u_1)$, is know, concepts from nonlinear elastic fracture mechanics can be applied to define the fracture behavior of a given structure. In the case of thin laminates it will be advantageous to describe the problem using beam/plate theory. The same approach can be formulated as an inverse problem to define the bridging law from indirect experimental measurements. A procedure has been proposed and successfully applied in [4] to define the Mode II bridging law, $p_1(u_1)$, of through-thickness stitches from crack profiles measurements

and load-deflection curves in ENF carbon/epoxy specimens. A similar approach is under formulation to define $\boldsymbol{p}(u_3,u_1)$ using the MMB test. Here some preliminary results will be presented which highlight the influence of the bridging mechanisms on crack growth.

Figure 4.b shows the system of loads applied to the MMB specimen if the weight of the lever is neglected (P is the load per unit width of the specimen applied to the rigid lever at a distance c from the center of the specimen). The external loads can be decomposed into their Mode I and Mode II components, $P_I=(3c/L-1)P/4$ (DCB type loading) and $P_{II}=(c/L+1)P$ (ENF type loading) [20]. The Mode I and Mode II components of the bridging tractions, $\boldsymbol{p}$, acting along the bridged portion of the crack are p_3 and p_1. In general p_3 and p_1 will depend on both u_3 and u_1.

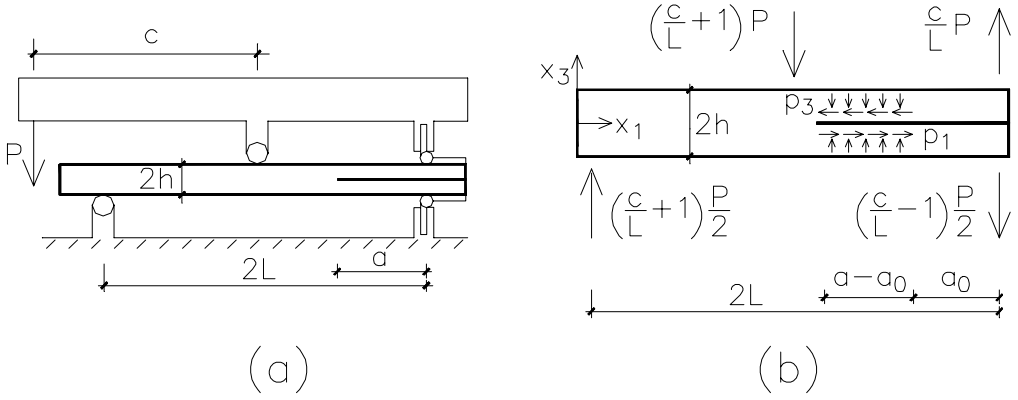

Fig.4: a) Mixed-Mode Bending test apparatus. b) Schematic of the Mixed-Mode Bending specimen with through-thickness reinforcements.

The strain energy release rate and the mode mixture are calculated using beam theory and the J-integral with an approach analogous to that presented in the previous section for the curved specimen (Eqs. 1, 4). In this phase classical beam theory has been used which assumes the rotations of the two delaminated arms of the specimen are equal at the delamination front. A corrected beam theory has been proposed in [17-19] for conventional (2D) laminates which accounts for relative rotations of the arms at the crack tip. In laminates reinforced through the thickness, however, the relative rotations at the tip are probably negligible due to the shielding effect provided by the closing tractions which tend to reduce the curvature of the arms. Further studies are required to verify this conjecture and to refine the model if necessary.

Due to the presence of the bridging mechanisms, the mode ratio, G_{II}/G_I, will depend on the value of the applied load, the crack length and the bridging law $\boldsymbol{p}(u_3,u_1)$. If p_3 and p_1 depend only on their respective crack displacements, u_3 and u_1, the strain energy release rate G is simply given by the superposition of the DCB and the ENF strain energy release rates [1-3,5]. To analyze crack propagation in the specimen a crack growth criterion is applied which assumes the crack to be at the onset of propagation when the strain energy release rate, $G=G_I+G_{II}$, becomes equal to a critical fracture energy $G_C = G_C(G_I,G_{II})$.

Figure 5 shows the dimensionless critical load, $P_{cr}/(E'_1 G_{IC} h)^{0.5}$ as a function of the normalized crack length, a/h, with E'_1 the reduced Young's modulus in the x_1 direction and G_{IC} the fracture energy of the unreinforced material when subject to pure Mode I loading. The material has been assumed as homogeneous and orthotropic and the specimen to be in plane

strain conditions normal to the axis x_2. The diagrams refer to a beam with an initial notch of length $a_0/h = 10$ and have been obtained by applying the fracture criterion $G_I/G_{IC} + G_{II}/G_{IIC} = 1$, with $G_{IIC} = 2\ G_{IC}$ the fracture energy of the unreinforced material under pure Mode II loading. This criterion has been suggested for unidirectionally reinforced polymer matrix laminates [6] but its validity on more general laminates is unproven and it is used here only as a first example of application. Constant bridging tractions have been assumed to act along the bridged crack, $p_3 = \alpha_3(E'_1 G_{IC}/h)^{0.5}$ and $p_1 = \alpha_1(E'_1 G_{IC}/h)^{0.5}$. Constant bridging tractions can give only a rough description of the bridging mechanisms of through-thickness reinforcement and they are used here in order to easily highlight the different mechanisms which develop during crack growth. The two diagrams of Fig. 5, (a) and (b), refer to two different loading systems which lead to mode ratios for unbridged delaminations equal to $G_{II}/G_I = 4$ and $G_{II}/G_I = 1$, respectively.

The dashed curves in each diagram depict the response of an unreinforced laminate: the critical load progressively decreases during crack growth while the mode ratio remains constant. The thick curves show the influence of through-thickness reinforcement on crack propagation. They have been obtained for $\alpha_1 = 0.2$ and by varying α_3 from 0.3 to 0.0 (these values might represent the average behavior of a typical stitched polymer matrix laminate with $E'_1 \approx 50$ GPa, $G_{IC} \approx 0.5$ N/mm, $h \approx 3$ mm). In all the cases the mode ratio G_{II}/G_I progressively increases during crack growth. The dotted curves in each diagram represent the response of an ENF specimen loaded in pure Mode II by P_{II}. When the thick curves reach the dotted curve G_I vanishes. For longer delaminations the specimen will be characterized by the presence of zones of contact behind the tip[1]. The response of the specimen in this phase has not been computed, however it is worth noting that the delamination can still propagate driven by the Mode II loading. Under certain conditions, which are not contemplated in Fig. 5, the sliding displacement can invert sign along portions of the crack during the monotonic loading process. The material will then be subject to local cyclic loadings.

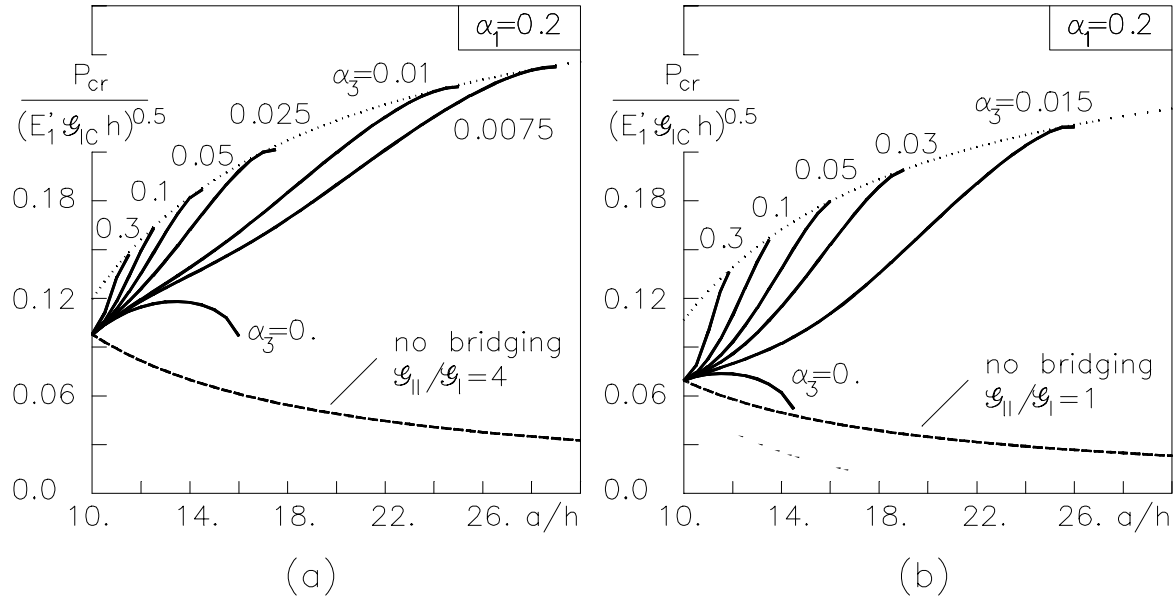

Fig.5: Critical load for crack propagation in the Mixed-Mode Bending specimen as a function of crack length (see assumptions in the text). a) $G_{II}/G_I = 4$ in the case of no bridging.
b) $G_{II}/G_I = 1$ in the case of no bridging.

[1] This is analogous to the oscillations of the vertical displacement found in the problem of a point load beam on an elastic foundation. It might be a common feature in delamination fracture specimens in the presence of large scale bridging, i.e. distributed linear or nonlinear foundation.

CONCLUSIONS

A beam theory formulation of the technologically important problem of a delamination crack driven through a curved structure by opening bending moments has been shown to be a very serviceable approximation in isotropic materials. The strain energy release rate and the mixture of Mode I and Mode II crack tip fields are accurately calculated, provided the curvature is not very large. Beam theory may also be reasonable for orthotropic materials, but only for cases of modest curvature. Generalized analytical results for the mode decomposition and stress intensity factors in delaminating curved beams have been derived, which may also be used to analyze crack propagation in finite element calculations of cases of general elasticity.

Modified beam theory is already known to provide an excellent description of the mixed mode bending specimen, which is being developed as a standard for measuring Mixed Mode fracture toughness in conventional (2D) laminates. Here a new formulation has been presented to deal with the large scale bridging effects of through-thickness reinforcement. With simple laws assumed for the bridging effects, some fundamental changes in crack behavior due to the through-thickness reinforcement have been demonstrated. For specimens of common dimensions, at a moderately large crack length and with a large bridging zone, the bridging tractions cause a rotation of the material in the near crack wake in response to Mode I loading, which shuts down the crack tip. The fracture surfaces come into contact at the crack tip and the Mode I energy release rate vanishes. In the absence of Mode II loading, the specimen must then necessarily fail by some mechanism other than crack propagation, e.g., failure of a loading arm or tensile or compressive failure under in-plane loads. If Mode II loading is present, crack propagation remains possible, but the Mode II shielding will be strongly modified by friction acting over the zones of contact. Contact appears to be very common in the simulations and clearly needs to be mapped out as a feature of the MMB test when dealing with laminates with through-thickness reinforcement. Another change in the behavior due to the through-thickness reinforcement regards the Mode II crack displacement. Under certain conditions the sliding displacement can change sign along portions of the crack during crack growth so that the material undergoes local cyclic loadings even when the process is globally monotonic.

Using a linear propagation criterion previously suggested for mixed mode cracking in unidirectional laminates, the critical stress for crack propagation has been illustrated for loads of various mode ratio. The resultant mode at the crack tip is strongly influenced by the large scale bridging effects. For crack growth from a notch, the critical load rises to that expected for pure Mode II loading as the mode ratio at the crack tip moves from that of the applied fields to that where the Mode I tip fields vanish. The extent of crack growth prior to reaching the Mode II limit will be of order of magnitude 10 – 100 mm in typical cases, depending on the bridging traction law, the notch size, and the laminate half-thickness.

ACKNOWLEDGEMENTS

The authors acknowledge support from the NATO (grant CRG.CRG 973062). RM was also supported by the Italian Dep. for the University and for Scientific and Tech. Research.

REFERENCES

1. Jain, L.K. and Mai, Y.-W., (1994), Analysis of stitched laminated ENF specimens for interlaminar Mode II fracture toughness, *Int. J. Fracture*, 68, 219-244.
2. Jain, L.K. and Mai, Y.-W., (1995), Determination of Mode II delamination toughness of stitched laminated composites, *Comp. Sci. and Tech*., 55, 241-253.
3. Massabò, R. and Cox, B.N., (1999), Concepts for bridged Mode II delamination cracks, *J. Mech. Phys. Solids*, in press.
4. Massabò, R., Mumm, D.R., and Cox, B.N., (1999), Characterizing mode II delamination cracks in stitched composites, *Int. J. Fracture*, in press.
5. Jain, L.K. and Mai, Y.-W., (1994), On the equivalence of stress intensity and energy approaches in bridging analysis, *Fatigue Fract. Engng Mater. Struct.*, 17, 339-350.
6. Reeder, J.R., and Crews, J.H., (1992), Redesign of the Mixed-Mode bending delamination test to reduce nonlinear effects, *J. Comp. Tech. & Research*, 14, 12-19.
7. Lu, T-J, Xia, Z.C. and Hutchinson, J.W., (1994), Delamination of beams under transverse shear and bending, *Materials Science and Engineering*, A188, 103-112.
8. Lu, T-J, Hutchinson, J.W., (1995), Role of fiber stitching in eliminating transverse fracture in cross-ply ceramic composites, *J. Am. Ceram. Soc.*, 78(1), 251-53.
9. Massabò, R., and Cox, B.N., (1999), Mixed Mode delamination in curved structures, submitted for publication.
10. Williams, J.G., (1988), On the calculation of energy release rate for cracked laminates, *Int. J. Fracture*, 36, 101-119.
11. Suo, Z., (1990), Delamination specimens for orthotropic materials, *J. Applied Mechanics*, 57, 627-634.
12. Lekhnitskii, S.G., (1968), *Anisotropic plates*, Gordon and Breach Science Publishers, NY.
13. Rice, J.R., (1968), A path independent Integral and the approximate analysis of strain concentration by notches and cracks, *J. Applied Mech*., 35, 379-386.
14. Baldacci, R., (1983), *Scienza delle Costruzioni*, vol.2., UTET, Torino (in italian).
15. Suo and Hutchinson, (1989), Steady-state cracking in brittle substrate beneath adherent films, *Int. J. Solids and Structures*, 25, 1337-1353.
16. Tada, H., Paris, P.C., and Irwin, G.R., (1985), *The stress analysis of cracks handbook*, Paris Production Inc., St. Louis, MO.
17. Kinloch, A.J., Wang, Y., Williams, J.G., and Yajla, P, (1993), The mixed-mode delamination of fibre composite materials, *Comp. Sci. and Tech*., 47, 225-237.
18. Wang, Y., and Williams, J.G., (1992), Corrections for Mode II fracture toughness specimens of composite materials, *Comp. Sci. and Tech*., 43, 251-256.
19. Williams, J.G., (1989), End corrections for orthotropic DCB specimens, *J. Comp. Tech. and Res.*, 35, 367-376.
20. Crews, J.H., and Reeder, J.R., (1988), A Mixed-Mode bending apparatus for delamination testing, *Nasa TM* 100662.